PAPER

Check for updates

Structural diversity in pyridine and polypyridine adducts of ring slipped manganocene: correlating ligand steric bulk with quantified deviation from ideal hapticity†

Anthony F. Cannella, [ID] [a] Suman Kr Dey,[a] Samantha N. MacMillan[b] and David C. Lacy [ID] *[a]

We have synthesized several new manganocene-adduct ([Cp$_2$Mn(L)] = **1**–L) complexes using pyridine and polypyridine ligands and report their molecular structures and characterization data. Consistent with other molecules in this class [(η^x-Cp)$_2$MnL$_n$] or [(η^x-Cp)$_2$Mn(L–L)] (n = 1, 2; x = 1, 3, or 5), the manganese-cyclopentadienide interaction deviates from the classical η^x interactions (x = 3 or 5). Such deviations have been ascribed to steric factors and often called non-ideal hapticity. However, there is no quantification of this non-ideal hapticity and thus it is difficult to evaluate the extent of ring slippage or assign hapticity. Furthermore, the hypothesis that non-ideal hapticity in high-spin Mn^{II} complexes is induced by steric interactions has not been systematically evaluated. Therefore, we report herein a quantified scale for deviation from ideal hapticity between zero (ideal η^5 interaction) and one ("η^1" interaction). This quantified deviation from ideal hapticity has an empirical relationship with the ligand's steric properties, which strongly supports the premise that steric interactions cause the deviations in ionic M–Cp interactions.

Introduction

Cyclopentadienide (Cp) is undoubtedly one of the most important ligands in organometallic chemistry. Since the discovery of its η^5 coordination to iron by structural means,[1] Cp is found as an auxiliary ligand in a variety of applications that include electron transfer studies,[2] asymmetric polymerizations,[3] and medicine.[4] One quality of Cp and related cyclic η^5-dienyl ligands is their ability to impact chemical reactivity by means of ring slip isomerization from a complex that has η^5 coordination to one that is η^3-allyl or monodentate ("η^1") and can even completely dissociate to form an outer sphere counter anion (Chart 1).[5] NMR spectroscopy is often used to reveal changes in hapticity because the dynamic nature of η^3-allyl Cp ligands makes them difficult to crystallize.[6] Known examples of structurally characterized complexes with *bona fide* haptotropic shifts display "ring folding", which indicates an authentic η^3-allyl binding mode.[7] An alternative form of isomeriza-

tion is called "ring slippage" which involves a change in hapticity of a Cp ring that remains planar. Veiros and coworkers have discussed the differences between folding and ring slippage showing that, in the latter case, the extent of slippage can be ambiguous and often described as non-ideal η^5 coordination (rather than η^3, *etc.*).[8]

This type of ring slippage is especially prevalent for manganese(II) cyclopentadienyl complexes because of the ionic nature of the Mn(II)–carbon bond.[9] For instance, the ionic character makes the Cp ligand in manganocene (Cp$_2$Mn = **1**) more labile[10] and susceptible to attack by an acid compared to other first row metallocenes.[11] Additionally, manganocene will form manganate anions to induce ring slippage by the addition of weak nucleophiles (*e.g.*, Cp) to the metal center.[12] Furthermore, the reaction of neutral monodentate (L) and bidentate (L–L) Lewis bases such as ethers,[13] carbenes,[14] amines,[15] and phosphines[16] with manganocene is also

[a]Department of Chemistry, University at Buffalo, State University of New York, Buffalo, New York 14260, USA. E-mail: dclacy@buffalo.edu
[b]Department of Chemistry and Chemical Biology, Cornell University, Ithaca, New York 14853, USA

†Electronic supplementary information (ESI) available. CCDC 1822539–1822546. For ESI and crystallographic data in CIF or other electronic format see DOI: 10.1039/c8dt00537k
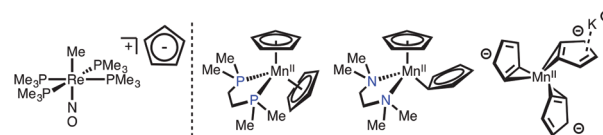

Chart 1 Diverse coordination chemistry of Cp anion.

reported to result in simple adducts of the type $[(\eta^5\text{-Cp})_2MnL]$ or $[(\eta^x\text{-Cp})_2Mn(L–L)]$ (x = 1 or 5) with ring slippage.

These ring slips are often accompanied by tilts of the planar Cp rings relative to the perpendicular axis. It has been shown that electronic arguments[17] do not apply to high-spin manganese(II) compounds and that steric factors are at play. Wilkinson, Hursthouse, and coworkers first forwarded this hypothesis for their high-spin 1-L and 1-L–L adducts, stating that electronic factors are likely a minor component to ring tilts because of negligible metal–ligand covalency.[16] Soon after this, Bottomley used the bond angles in 1-THF to show that steric factors were indeed responsible for the observed ring tilts.[13] The factors that result in slippage are therefore likely to also be steric in nature. More recent observations made by Walter, Wright, and Layfield for their Cp$_n$Mn-L (n = 1,2) type complexes also deviate from ideal η^5 coordination and provide further support for this ionic model.[18] Finally, the chelating diphosphine and diamine ligands dmpe (dmpe = 1,2-bis(dimethylphosphino)ethane) and TMEDA (TMEDA = $N,N,N'N'$-tetramethylethylene-1,2-diamine) have both been used to prepare 1-(L–L) compounds. The 21 electron 1-dmpe complex contains two nominal η^5-Cp ligands, whereas the 17 electron 1-TMEDA complex contains one η^5-Cp ligand and one η^1-Cp ligand.[15,16] Tertiary amine ligands are more bulky than their phosphine congeners and further demonstrate the effects of steric bulk in these otherwise similar molecules.

Additional compounds with varying degrees of hapticity are required to confirm the role of steric effects in ring slip and to gather guiding principles to control the extent of slippage. Herein, we describe the synthesis and characterization of additional compounds of the 1-L class using mono-, di-, and tridentate (poly)pyridine ligands. Using these new compounds and data from an extensive list of known manganocene adducts, we structurally parameterize the deviation from ideal η^5 coordination in this family of compounds. In doing so, a strategic method to control ring slip has emerged in addition to providing a novel method to empirically evaluate the steric bulk of neutral ligands.

Results

Synthesis and characterization of the 1-L adducts

The [Cp$_2$Mn-L] adducts (1-L) were synthesized by mixing Cp$_2$Mn (1) and the desired ligand (L) in a 1 : 1 stoichiometry in THF at room temperature (Scheme 1). The 1-L adducts were purified by crystallization from THF or toluene at −35 °C and afforded crystals suitable for diffraction. We attempted to synthesize the mono-, di-, and tri-pyridine adducts 1-py$_n$ (n = 1, 2, and 3) by adding the corresponding equivalents of pyridine to 1, but we only obtained 1-py$_2$ for all three reactions. The compounds are not indefinitely stable and therefore prepared fresh in small batches and stored in the crystallization mother liquor. The combustion CHN analysis of week-old samples or samples dried extensively under vacuum provided carbon percentages substantially lower than expected. Only when samples were freshly prepared and washed sparingly with cold petroleum
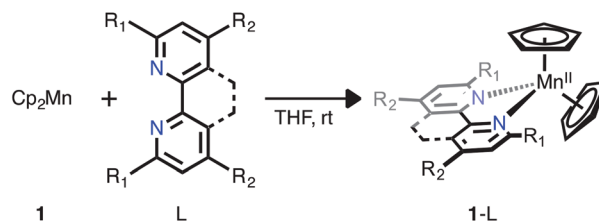
Scheme 1   Synthesis of Cp$_2$Mn (1) adducts: L = 2,2′-bipy (bipy, R_1 = R_2 = H); 4,4′-Me$_2$bipy (R_1 = H, R_2 = Me); 6,6′-Me$_2$bipy (R_1 = Me, R_2 = H); 6,6′-Ph$_2$bipy (R_1 = Ph, R_2 = H); 1,10-phenanthroline (phen, R_1 = R_2 = H); 4,7-Ph$_2$phen (R_1 = H, R_2 = Ph); 2,9-Me$_2$phen (R_1 = Me, R_2 = H); py$_2$ (py = pyridine); terpy (terpyridine).

ether, dried open to the glovebox nitrogen atmosphere, and finally sealed in briefly evacuated glass ampules were we able to obtain reliable CHN analysis for most of the compounds. The instability and difficulty associated with obtaining reliable CHN for these 1-L adducts was also encountered by Howard et al. for 1-PR$_3$ (PR$_3$ = PMePh$_2$, PMe$_3$, dmpe).[16]

THF solutions of 1 are colorless, but the 1-L adducts complexes are yellow or red in THF. The UV-vis spectra of 1-L are generally featureless save for intense bands in the UV region associated with ligand π–π* transitions and ill-defined bands in the visible region that are likely CT in nature owing to the fact that ligand field transitions in high-spin Mn(II) are spin forbidden (Fig. S1†). A similar color change from colorless to red was observed when 1 was treated with 6,6′-diphenylbipyridine in THF. However, attempts to isolate and characterize 1-6,6′-2,2′-diphenylbipyridine only resulted in the isolation of free ligand and 1.

The magnetic properties of the adducts were explored with EPR and Evans' method. The solution state magnetic moments for some of the adducts were determined in benzene, but low solubility and relative instability of the complexes precluded most of the compounds from being measured. In the instances where data were collected, the values were near those expected for high-spin 1 complexes (μ_{eff} = 6.1μ_B for 1-2,9-Me$_2$phen). The EPR spectra at low temperature (6–15 K) exhibit features nearly identical to free manganocene (Fig. S1†). Overall the conclusion is that the compounds exhibit high-spin electronic configurations that are well within the expectations for most organometallic Mn(II) complexes.

Molecular structures of the 1-L adducts

The 1-L complexes exhibit typical binding modes between the metal center and the polypyridine ligand (Fig. 1). However, the Cp–Mn interaction varies depending on the polypyridine ligand and is the subject of the remainder of this manuscript. The 1-L adducts crystallized in a variety of space groups and often contained multiple molecules per asymmetric unit (Fig. S2–S9†). For instance, the asymmetric unit of 1-bipy contained three molecules of the form [Cp$_2$Mn(bipyridine)] and each of these three molecules have their own unique bond metrics and are therefore treated separately in our analysis.

In order to rationalize the observed structural diversity in the 1-L adducts we operationally define several key structural
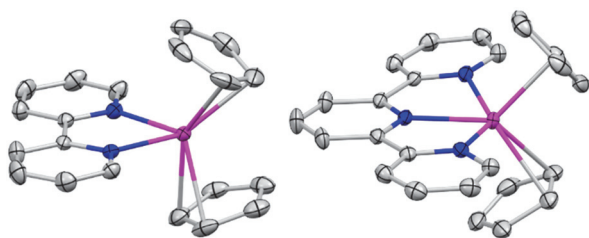
Fig. 1 Molecular structure of one of the molecules in the asymmetric unit for compounds **1**-bipy (left) and **1**-terpy (right); ellipsoids shown at 50% probability and solvent molecules and H-atoms in the crystal structure are not displayed. Atom colors: grey = C; blue = N; magenta = Mn. See Fig. S2−9† for remaining molecular structures.
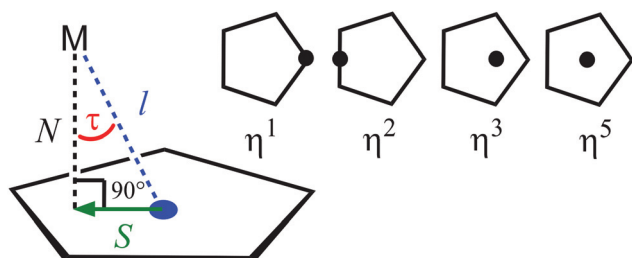
Fig. 2 Geometric parameters used in this study (left) and traditional binning of hapticity (right).

components (Fig. 2). The first of these important metrics that describe the **1**-L complexes is the Mn–Cp$_{centroid}$ distance (l) (each complex having two values of l) and is defined as the distance from the Mn ion to the center of the Cp ring (M–Cp$_{centroid}$ distance). The slip parameter (S)[19] for planar Cp rings, a characteristic of all the Cp rings studied here, is defined as the distance from the Cp$_{centroid}$ to a point on the Cp ring that coincides with a normal vector (N) from the metal ion to the plane of the Cp ring. The slip metric S forms the short edge of a right triangle with l as the hypotenuse and N as the second largest length. The angle between l and N is thus the tilt angle (τ) and is easily obtained by using the sine law as shown in eqn (1).

$$\tau = \sin^{-1}\left(\frac{S}{l}\right) \qquad (1)$$

These three parameters (l, S, and τ) provide the major points of interest from which the different **1**-L adducts are compared. For example, **1**-6,6′-Me$_2$bipy has l = 2.360 and 2.438 Å, S = 0.464 and 0.858 Å, and τ = 11.33° and 20.61°. These are quite different from the simple **1**-THF with l = 2.164 Å, S = 0.093 Å, and τ = 2.47°. A complete list of these metrics for the complexes that we synthesized and related compounds from the literature is summarized in Table 1.‡

‡ Table 1 is available as an excel file; please contact corresponding author: dclacy@buffalo.edu.

Discussion

Single crystal X-ray diffraction analysis reveals that each of the eight new **1**-L adducts contain typical coordination between the metal ion and the (poly)pyridine ligand but have ambiguous hapticity Cp ligation. A notable characteristic is the diversity in the coordination of the Cp rings that manifest in a degree of ring-slippage (S), M–Cp$_{centroid}$ distance (l), and tilts (τ) from complex to complex (Fig. 2). Upon initial inspection, there was no obvious trend between the (poly)pyridine ligand in **1**-L and the extent of ring-slippage except that the **1**-terpy adduct contains the largest M–Cp$_{centroid}$ distance. A correlation was indeed found between the steric bulk of the ligand and the extent of ring-slippage, but this required a quantification of the extent of hapticity change in addition to quantification of the ligand steric bulk, each of which is described in the following sections. The Tolman cone angle (Θ_T) and buried volume parameters (%V_{bur}) have been extensively used and conveniently defined and therefore constitute our preferred choices in parameterizing the adduct ligand. Finally, in addition to the eight new compounds synthesized and characterized herein, we also compiled the important bond metrics for all of the known relevant manganocene adduct complexes (Table 1) to effectively discover a correlation with our new non-ideal hapticity parameter and the steric bulk of the ligands.

Non-idealized hapticity parameter (*D*)

The M–Cp interaction, l, in the **1**-L adducts does not fall into idealized hapto environments (η^5, η^3, η^2, or η^1, Fig. 2) and, at first glance, does not appear to follow any trend, nor was there any evidence that electronic factors are at play. We are not the first to notice this seemingly ambiguous interaction, which has been described before as non-idealized η^5 interactions and attributed to steric factors.[13,16,18] Prior to this report, a systematic evaluation of this proposal was not possible and therefore we formulated a new parameter, D, that quantifies the deviation from idealized hapticity. For a given system of compounds, this value D is defined by eqn (2),

$$D = \frac{x - x_{min}}{x_{max} - x_{min}} \qquad (2)$$

where x is some geometric value, or a metric that is determined from geometric values, measured from X-ray crystal structures. At the onset, it was not obvious which geometric value or metric to use for the calculation of D. To solve this issue, we independently quantified the steric bulk properties of the adduct ligand Θ_T and %V_{bur} and plotted them against various geometric values or metrics. These are discussed later, but briefly here we found that the best correlation of D was obtained using the metric $l \times N$ for the value of x in eqn (2). The restriction of S to inside the Cp ring creates a relationship between N and l for which $l \times N$ is a metric (meaning a calculated-measurement). Hence, eqn (2) uses $(l \times N)_{min}$ as the minimum observed value found for the centroid distance multiplied by its corresponding N among the

Table 1 Crystallographic and geometric parameters for manganocene adducts[a]

Entry	Complex		l^g (Å)	D	D_{avg}	τ (°)	S (Å)	N (Å)	M–L (Å)	Avg Θ_T (°)[c]	Avg %V_{bur}[d]	Ref.[e]
1	1-THF		2.164	0.133	0.133	2.47	0.093	2.162	2.226	104.15	17.4	13
2	1-PMe₃		2.179	0.000	0.136	22.02	0.817	2.020	2.577[f]	101.41	19.0	16
			2.238	0.272		7.27	0.283	2.220				
3	1-PPh₂Me		2.236	0.251	0.222	10.00	0.388	2.202	2.612[f]	122.91	22.0	16
			2.194	0.194		3.46	0.132	2.190				
4	1-dmpe		2.334	0.475	0.475	8.22	0.334	2.310	2.674[f]	(184.71)	31.8	16
5	1-TMEDA		2.791	0.946	0.598	35.12	1.605	2.283	2.354	100.96	38.9	15
			2.222	0.250		4.55	0.176	2.215	2.338	(201.93)		
6	1-(TMG)₂		2.708	0.925	0.859	30.35	1.368	2.337	2.119[f]	132.96	21.0	18a
			2.615	0.792		27.76	1.218	2.314	2.109[f]	(265.91)	(41.3)	
7	1-(BzEDA)		2.205	0.217	0.556	3.45	0.133	2.201	2.226	103.44	37.9	18b
			2.744	0.895		33.70	1.522	2.283	2.261	(206.88)		
8	1-(NHC^ArMe2Br)		2.219	0.206	0.385	11.24	0.430	2.177	2.227	154.08	29.7	14a
			2.439	0.565		17.99	0.848	2.287				
9	1-IMes		2.212	0.193	0.388	10.91	0.419	2.172	2.222	159.21	30.3	14a
			2.445	0.583		20.04	0.838	2.297				
10	1-(NHC^Me4)₂		2.683	0.920	0.960	28.63	1.285	2.355	2.214	151.19	23.7	14a
			2.704	1.000		27.52	1.249	2.398	2.219	(302.38)	(46.7)	
11	1-IiPrMe₂		2.300	0.353	0.353	13.86	0.551	2.233	2.159	151.62	26.6	14b
			2.300	0.353		13.86	0.551	2.233				
12	1-ItBu		2.251	0.320	0.504	0.00	0.000	2.251	2.222	—	34.9	14b
			2.553	0.688		26.49	1.139	2.285				
13	1-IMes		2.425	0.552	0.372	19.28	0.801	2.289	2.225	156.07	30.3	14b
			2.211	0.191		10.92	0.419	2.171				
14	1-bipy[b]	Mn1	2.293	0.376	0.364	9.58	0.382	2.261	2.243	91.59	30.8	This work
			2.275	0.336		9.77	0.386	2.242	2.251	(183.18)		
		Mn2	2.326	0.386		15.81	0.634	2.238	2.236			
			2.310	0.413		9.55	0.383	2.278	2.222			
		Mn3	2.278	0.341		9.91	0.392	2.244	2.232			
			2.262	0.331		5.65	0.223	2.251	2.257			
15	1-4,4′-Me₂bipy		2.397	0.516	0.413	17.58	0.724	2.285	2.223	91.91	30.9	This work
			2.291	0.310		15.93	0.629	2.203	2.217	(183.82)		
16	1-6,6′-Me₂bipy		2.360	0.509	0.533	11.33	0.464	2.314	2.233	114.72	37.2	This work
			2.438	0.558		20.61	0.858	2.282	2.254	(229.44)		
17	1-phen[b]	Mn1	2.514	0.645	0.452	24.64	1.048	2.285	2.218	91.18	30.6	This work
			2.277	0.338		10.06	0.398	2.242	2.212	(182.37)		
		Mn2	2.363	0.494		13.47	0.550	2.298	2.262			
			2.281	0.332		11.77	0.465	2.233	2.253			
18	1-2,9-Me₂phen[b]	Mn1	2.391	0.506	0.509	17.37	0.714	2.282	2.255	115.78	36.7	This work
			2.336	0.496		5.30	0.216	2.326	2.251	(231.55)		
		Mn2	2.412	0.580		15.35	0.638	2.326	2.244			
			2.378	0.454		18.96	0.773	2.249	2.253			
19	1-4,7-Ph₂phen		2.330	0.436	0.436	12.01	0.485	2.279	2.227	91.17	30.7	This work
			2.330	0.436		12.01	0.485	2.279	2.227	(182.35)		
20	1-py₂		2.478	0.604	0.604	22.82	0.961	2.284	2.210[f]	114.99	18.6	This work
			2.478	0.604		22.82	0.961	2.284	2.210[f]	(229.98)	(36.6)	
21	1-terpy[b]	Mn1	2.703	0.882	0.786	31.37	1.407	2.308	2.238	125.17	42.1	This work
			2.524	0.741		21.09	0.908	2.355	2.355	(250.34)		
		Mn2	2.796	0.995		34.11	1.568	2.315	2.282			
			2.396	0.563		13.88	0.575	2.326	2.371			
		Mn3	2.620	0.808		27.59	1.214	2.322	2.239			
			2.503	0.726		19.25	0.825	2.363	2.357			

Abbreviations: l = Mn–Cp$_{cent}$ distance (Å); D = non-idealized hapticity parameter; D_{avg} = average of the values of D for a given complex; adduct Θ_T = Tolman cone angle of the adduct (°); %V_{bur} = percent buried volume of the adduct; τ = tilt angle (°); S = magnitude of slip vector (Å); N = normal vector from Mn to the plane of the Cp ring. [a] See Fig. 2 for the definition of parameters. [b] Asymmetric unit contains multiple molecules and is designated as Mn1, Mn2, etc. [c] As determined in this work: steric ligand angles (Θ_T) were determined from crystallographic parameters using eqn (3) and (4). Cone angles in parentheses are Θ_T multiplied by two (see Discussion). [d] As determined in this work: values in parenthesis are %V_{bur} calculated using both monodentate ligands as a single entity. The Θ_T and %V_{bur} for compounds with multiple molecules in the crystallographic unit cell are reported as the average value. [e] References are for crystallographic information only. [f] M–L distance is outside one standard deviation (0.109 Å) of the average M–L distance (2.267 Å) and thereby give potentially erroneous Θ_T. Ligand abbreviations: dmpe = 1,2-bis(dimethylphosphino)ethane; TMEDA = tetramethylethylenediamine; TMG = 1,1,3,3-tetramethylguanidine; BzEDA = N_1,N_2-dibenzylethane-1,2-diamine; NHC^ArMe2Br = 1,3-bis(2,6-dimethyl-4-bromophenyl)-imidazol-2-ylidene; NHC^Me4 = 1,3,4,5-tetramethylimidazol-2-ylidene; IMes = 1,3-dimesitylimidazol-2-ylidene; IiPrMe₂ = 1,3-diisopropyl-4,5-dimethylimidazol-2-ylidene; ItBu = 1,3-di-$tert$-butylimidazol-2-ylidene. [g] esd ≤ 0.002 Å.

1-L adducts, and $(l \times N)_{max}$ is the maximum observed value found for the centroid distance multiplied by its corresponding N among the **1**-L adducts. The D parameter is, by nature, a comparative metric and must be defined by a specific set of compounds bounded by the two most extreme examples. Complex **1**-PMe₃ has the smallest $l \times N$ value and

was used for the idealized η^5 interaction with a D value equal to zero for one of the Mn–Cp interactions (Table 1, entry 2). On the other end of the spectrum, the maximum deviation from idealized hapticity is defined as essentially having a so-called η^1 interaction. The largest value of $l \times N$ observed among any known **1**-L complex is for one of the M–Cp interactions in **1**-NHC$^{Me4}_2$ (Table 1, entry 10). One of the Mn–Cp interactions in **1**-terpy is a near second to a maximum deviation with a D value of 0.995 (Table 1, entry 21). One can also take the average for all the D values (D_{avg}) for each of the different M–Cp interactions in a single compound. The D_{avg} parameter actually serves as the more meaningful parameter with which the steric parameters are correlated because the adduct ligand affects both Cp rings simultaneously (*vide infra*).

Cone angle

The ligand cone angle (Θ_T) was developed by Tolman to para-meterize phosphine steric bulk.[20,21] This was done using 3D molecular models and projecting a cone from the metal center with boundaries defined by the outermost van der Waals radii
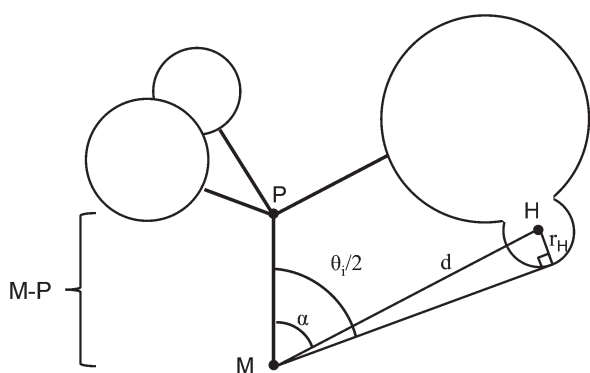
Fig. 3 Schematic of geometric entities required for calculation of a cone angle for a phosphine ligand; figure adaptation from the Tolman and Mingos' reports defining cone angles.[21,22]

on the ligand. To calculate a full cone angle Θ_T, Tolman utilized eqn (3),

$$\Theta_T = \frac{2}{i} \sum_i \left(\frac{\theta_i}{2} \right) \tag{3}$$

where the "half angles" ($\theta_i/2$) are the angles formed from the metal–phosphine bond and outermost van der Waals radii for the i_{th} substituent (Fig. 3).

Mingos and coworkers later developed a method to obtain the cone angle directly from crystallographic parameters, which included the H-atom van der Waals radii.[22] The half angle determined by Mingos' method requires eqn (3) and (4),

$$\frac{\theta_i}{2} = \alpha_{Mingos} + \frac{180}{\pi} \sin^{-1}\left(\frac{r_H}{d} \right) \tag{4}$$

where α and d are the parameters that can be obtained directly from the crystal structure (Fig. 3). The H-atom van der Waals radii are 1.0 Å in C–H bonds, which are relevant here.[22,23]

Since eqn (3) does not mathematically describe a three-dimensional shape, we can use the same formulae (eqn (3) and (4)) to calculate a two-dimensional "cone" angle (also designated Θ_T for convenience) for planar monodentate ligands such as THF and pyridine. Tolman restricted the value of i from 1–3, but Walter and coworkers effectively used values of i from 1–5 to determine the cone angles of Cp ligands (Θ_W, Table 2).[24] Hence, the value of i for THF and pyridine is simply two instead of three. Unfortunately, the lack of three-dimensional information in Θ_T negatively impacts the comparative value between ligands such as THF and PPh$_2$Me. Later, this issue is resolved using percent-buried volume (*vide infra*).

Many of the ligands used in this study are multidentate and afford a different problem from which to draw meaningful comparisons. The historical way to report Θ_T for multidentate ligands is to use eqn (3) with one of the $\theta_i/2$ being half of the bite angle and the other $\theta_i/2$ defined by the bound atom and van der Waals radii of the outermost atom determined the same way for phosphine ligands according to eqn (4) (Fig. 4).

Θ_T determined this way provides the cone angle for one side of a bidentate phosphine. A plot of D_{avg} *vs.* Θ_T does not

Table 2 Comparison of DFT calculated and XRD obtained l_{avg}, adduct Θ_T, Cp Θ_W, and %V_{bur}

1-L Ligand	l_{avg} (Å)^a			Adduct Θ_T (°)			Cp Θ_W (°)^a			%V_{bur}		
	DFT	XRD	|diff|^b	DFT	XRD	|diff|^b	DFT	XRD	|diff|^b	DFT	XRD	|diff|^b
bipy	2.338	2.291	0.047	187.00	183.18	3.82	87.70	85.56	2.14	30.0	30.8^c	0.8
6,6′-Me$_2$bipy	2.391	2.534	0.143	227.80	229.45	1.65	86.28	82.58	3.70	36.1	37.2	7.1
6,6′-Ph$_2$bipy^e	2.334			233.51			88.02			33.8		
4,4′-Me$_2$bipy	2.350	2.345	0.004	186.87	183.81	3.06	87.46	83.61	3.85	30.1	30.6	0.5
phen	2.317	2.359	0.043	184.00	182.37	1.63	88.41	84.23	4.18	29.4	30.9	1.5
2,9-Me$_2$phen	2.398	2.38	0.018	227.36	231.55	4.19	86.07	83.08	2.99	36.0	36.7	0.7
4,7-Phphen	2.320	2.331	0.011	184.99	182.35	2.64	88.08	84.51	3.57	29.8	30.7	0.9
py$_2$	2.525	2.479	0.046	237.87	229.98	7.89	82.44	80.57	1.87	35.8	36.6	0.8
terpy	2.644	2.591	0.052	255.84	250.34	5.50	79.58	78.10	1.48	41.9	42.1^d	0.2
		0.046 ± 0.043			3.797 ± 2.106			2.973 ± 1.016			0.8 ± 0.4	

^{a} The Cp cone angle provided (Θ_W) is average of both M–Cp interactions.[24] ^{b} Absolute value of the difference of DFT–XRD. ^{c} NiBr$_2$**bipy** = 35.7 ^{d} Ru (H$_2$O)(bipy)(**terpy**) = 47.7.[25] ^{e} The adduct **1**-6,6′-Ph$_2$bipy could not be isolated.
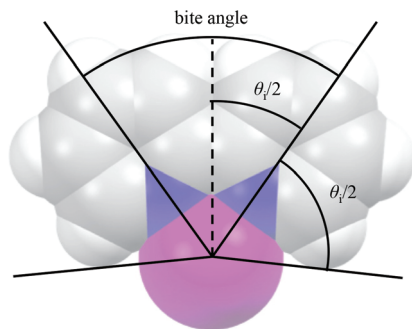
Fig. 4 Geometric location of half angles ($\theta_i/2$) for planar multidentate ligands.

correlate when the traditional Θ_T used for bidentate ligands is used (Fig. 5, blue dots). However, a linear correlation (R^2 = 0.93) is obtained when one plots D_{avg} vs. Θ_T in which all of the multidentate and bis(monodentate) ligands are multiplied by two. Hence, Θ_T for multidentate ligands and complexes with more than one of the same monodentate ligands (e.g., **1**-py$_2$) were summed in order to fully account for the steric bulk of the ligand; these summed Θ_T are reported in Table 1 in par-
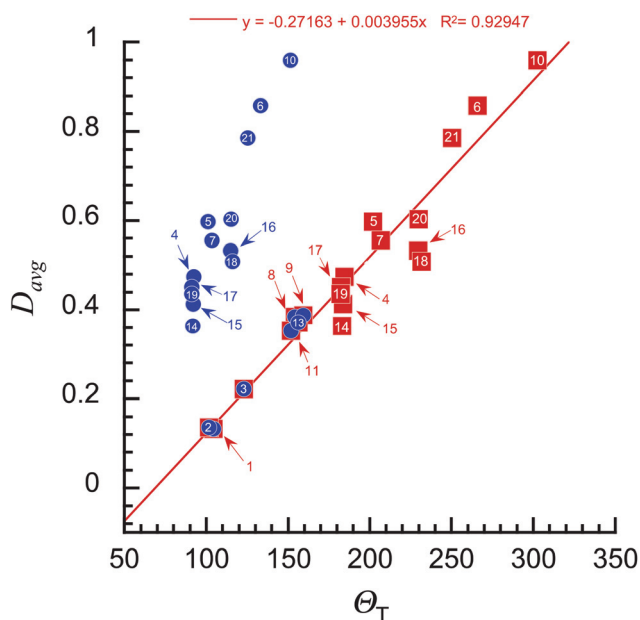

Fig. 5 A plot of the deviation from idealized hapticity (D_{avg}) versus the Tolman cone angle (Θ_T). The circles represent data points with Θ_T values determined directly from eqn (3) and (4). The squares represent data points with Θ_T values determined from eqn (3) and (4) but also take into consideration both halves of multidentate ligands (e.g., bipy) or twice the value for compounds with two monodentate ligands (e.g., pyridine). The inscribed numbers correspond to the entries in Table 1. The red line is a linear regression fit for the square data points and is shown to highlight the trend (R^2 = 0.93). The D_{avg} value (Table 1) was obtained by taking the average of all Mn–Cp interactions in a unit cell for a given compound's crystal structure (e.g., a D_{avg} value for a compound in which the crystal structure contains three molecules is the average of six Mn–Cp D values). The same operation was performed for Θ_T.

entheses. The correlation between deviations from idealized hapticity (D_{avg}) and the steric bulk (Θ_T) is intuitive, with the largest ligands showing the largest deviation from idealized hapticity (Fig. 5).

The D_{avg} parameter provides a substantially better correlation when $N \times l$ is used for the metric in eqn (2) than with other geometric parameters or metrics. For instance, a plot of D_{avg} that uses the average tilt angle (τ) or the average magnitude of the slip vector (S) versus the steric properties of the ligand have poor correlations (Fig. S10 and Table S2†). Despite the poor relationships, there are still observable trends in these complexes with bulkier ligands having larger average S or τ values.

Finally, it is also important to discuss the effect of M–L distance on the value of Θ_T. Tolman standardized the M–P distance to 2.28 Å and found that deviations in M–P distances of 0.1 Å only changed Θ_T by ≤5°.[21] Mingos explored the relationship between M–P and Θ_T and showed that the average of many Θ_T for M–PPh$_3$ complexes determined using the crystallographic M–P distance was statistically equivalent to the Θ_T determined by Tolman. Nonetheless, Mingos demonstrated that a large spread of Θ_T values exists over the full range of M–P distances. Conveniently, the **1**-L adducts studied here have an average M–L bond distance of 2.267 Å with a standard deviation of 0.109 Å, very close to the standard 2.28 Å used for conventional Θ_T and hence there is no need to standardize the M–L distances in this study. Some of the M–L distances do fall outside one standard deviation of the M–L distances investigated here and these are indicated in Table 1 with footnote f.

While the trend between D_{avg} and Θ_T reveals a correlation between steric bulk and deviation from ideal hapticity, the comparison has some shortcomings. First, D_{avg} varies between molecules of the same compound and suggests that other factors, such as crystal packing, are at play. To address this issue, we used density functional theory to optimize the **1**-L adducts and compare the computed values of D and compare them to the experimental values. We also used the optimized geometries to determine Θ_T for the adducts. These results are summarized in Table 2 and show that the computational results match closely to the experimental values. The small deviations from DFT and XRD are probably due to subtle crystal packing effects.

Percent buried volume

A second shortcoming in the D_{avg} and Θ_T comparison results from the failures of Θ_T, which are a lack of three-dimensional information and its inability to address changes in the M–L distance. Attempts in the scientific community to find a more inclusive steric parameter have led to the discovery and application of the percent buried volume (%V_{bur}) parameter.[26]% V_{bur} is defined as the space occupied by the ligand in the first coordination sphere of the metal center and has since been shown to correlate well with a variety of chemical properties including reactivity.[27] The primary advantage of %V_{bur} over Θ_T is that it can be universally applied and compared across all types of M–L interactions with the freeware SambVca.[25]

Cavallo and coworkers found that a sphere radius of 3.5 Å provided the best fit for a large collection of ligands that included phosphines and N-heterocyclic carbenes. This insight made by Cavallo and Nolan is that since a majority of M–L bond distances fall within the range of 2.0–2.5 Å, a sphere radius of 3.5 Å is sufficient to account for the van der Waals radius of the atoms directly coordinating to the metal center in most cases. Proceeding with the same method outlined by Cavallo and coworkers using SambVca we calculated the $\%V_{bur}$ of the ligands in the **1**-L adducts relevant to this work (Table 1) and used the same program to generate steric maps for the ligands (Fig. 6).[28] Additionally, we compared the $\%V_{bur}$ determined from the XRD and those of the DFT computed structures for the new eight **1**-L adducts described herein (Table 2). The deviation from ideal hapticity correlates well with the $\%V_{bur}$ determined for the **1**-L adducts with an essentially equal correlation compared to Θ_T (Fig. 7, $R^2 = 0.92$).

For complexes with multiple monodentate ligands (*e.g.* **1**-py$_2$), the $\%V_{bur}$ was determined for a single ligand in addition to both ligands as a single entity, just as it was performed for the Θ_T values (Table 1). For example, the $\%V_{bur}$ of one of the pyridine ligands in **1**-py$_2$ is 18.6%, but if one includes both pyridine ligands the $\%V_{bur}$ is 36.6%. The correlation shown in Fig. 7 uses the $\%V_{bur}$ for both ligands as a single entity, as they are both contributing to the overall steric bulk causing ring slip. We note that the $\%V_{bur}$ of pyridine in **1**-py$_2$ (18.6%, entry 20) is very close to other monodentate ligands such as the single THF ligand **1**-THF (17.4%, entry 1), NHC^{Me4} in **1**-(NHC^{Me4})$_2$ (23.7%, entry 10), and TMG in **1**-TMG$_2$ ($\%V_{bur}$ 21.0%, entry 6). Why the smallest ligand in this list is the only **1**-L adduct with a single monodentate ligand is uncertain. We attempted to synthesize the mono and tris pyridine adduct of **1** but only **1**-py$_2$ was isolated from these reactions.
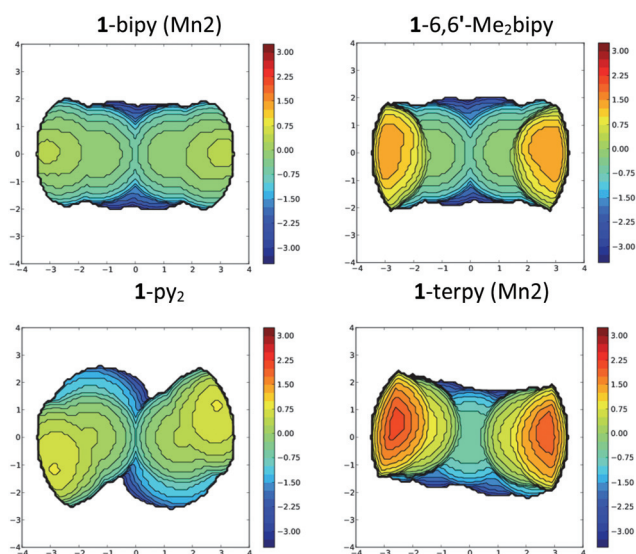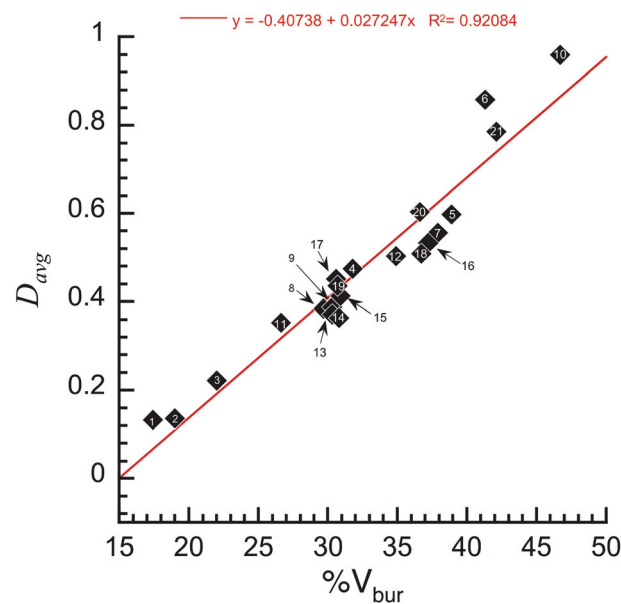

Fig. 7 A plot of the deviation from idealized hapticity (D_{avg}) *versus* the $\%V_{bur}$. The red line is a linear regression fit to the data shown ($R^2 = 0.92$). The inscribed numbers correspond to the entries in Table 1. The D_{avg} value (Table 1) was obtained by taking the average of all Mn–Cp interactions in a unit cell for a given compound's crystal structure (*e.g.*, a D_{avg} value for a compound in which the crystal structure contains three molecules is the average of six Mn–Cp D values). The same operation was performed for $\%V_{bur}$.

Conclusions

We have confirmed that Cp ring slippage in manganocene adducts is the result of steric factors by correlating the steric bulk of the coordinating ligand and the extent of ring slippage. This required a defined non-ideal hapticity parameter (D) for which we are the first to execute and did so by compiling our own and most other known adducts relevant to the current work. The correlations between the deviation from ideal hapticity (D_{avg}) and the steric bulk, either Θ_T or $\%V_{bur}$, of the adduct ligand clearly demonstrate that steric effects are the predominant forces causing the ring slip in ionic metallocenes. Additionally, the similarity with DFT calculated values (D, Θ_T, Θ_W, $\%V_{bur}$) shows that crystal-packing effects are minor in causing ring slip. This brings about an interesting possible application of the correlation that we have found in that a predictable degree of ring slip can be designed into an ionic metallocene by tuning the steric bulk. Considering the importance of molecular structure in controlling the properties of catalysts or single molecular magnets, this type of structural control could potentially find application in a variety of fields where cyclopentadienide ligands are employed.

Experimental

General methods

All manipulations were performed under a dry, anaerobic argon atmosphere using Schlenk line techniques or in a nitro-

Fig. 6 Representative steric maps for **1**-L adducts. The *x*-axis and left *y*-axis are in units of Å. See Fig. S11 and S12† for remaining maps.

gen-filled VAC Atmosphere Genesis glovebox. The reagents were purchased from commercial vendors and used without further purification unless otherwise specified. Terpyridine, 4,7-diphenyl-1,10-phenanthroline, and 4,4′-dimethyl-2,2′-bipyridine were generously donated by Professor Jim Atwood (University at Buffalo). 3 Å molecular sieves were activated by heating ≥ 200 °C under vacuum (≈100 mTorr) for 48 h. Anhydrous solvents were purified using a Pure Process Technology solvent purification system and stored in a glovebox over 3 Å molecular sieves for at least 24 h before use. ^{1}H NMR spectra were recorded on a Varian Mercury-300 or Varian Inova-400 MHz spectrometer. The values of chemical shifts (ppm) are referenced to the residual solvent proton resonances. UV-vis spectra were collected using an Agilent Cary 8454 spectrophotometer. Solid ATR-FTIR spectra were collected inside of an argon filled Omni VAC glovebox using a Bruker Alpha IR spectrophotometer (PLATINUM-ATR insert module). The synthesis of MnCp$_2$ was performed according to the published protocol[11] except that NaH, rather than Na metal, was used to prepare NaCp.

Synthesis of 6,6′-diphenyl-2,2′-bipyridine. This procedure is modified after a literature report for 6,6′-dimesityl-2,2′-bipyridine.[29] To a toluene suspension (30 mL) of 6,6′-dibromo-2,2′-bipyridine[30] (0.433 g, 1.38 mmol), an excess of phenylboronic acid (0.505 g, 4.14 mmol, ≥97% HPLC grade) dissolved in 5 mL of dimethylformamide (DMF) was added. A 10 mL sample of 2 M Na$_2$CO$_3$, Pd(OAc)$_2$ (2 mol%), and triphenylphosphine (10 mol%) were added to the reaction flask and the reaction mixture was refluxed for 24 h open to air, cooled to room temperature, and allowed to settle to separate the aqueous and organic layers. The organic layer was washed with brine (3 × 100 mL) and the aqueous layer was washed with chloroform (3 × 100 mL) and the organic fractions were combined and reduced to an oil on a rotary evaporator. The oil was triturated with 30 mL hexane and the resulting solid was filtered and washed with water (3 × 15 mL) and hexanes (3 × 10 mL) and dried overnight under vacuum (product does sublime). Spectroscopic data matches the literature (CDCl$_3$).[31]

Synthesis of 1-bipy. A solution of MnCp$_2$ (95 mg, 0.51 mmol) in THF (5 mL) was added dropwise to a solution of 2,2′-bipyridine (76 mg, 0.49 mmol) in THF (5 mL) at room temperature. The reaction mixture turned dark red/brown and was stirred at room temperature for 45 minutes and then recrystallized by storing at −35 °C. The crystals obtained at −35 °C were filtered cold and washed once with 5 mL of cold petroleum ether (117 mg, 70%). Saturated solutions of the adduct in toluene stored at −35 °C afforded XRD quality crystals. UV-vis (THF, nm (ε, M^{-1} cm^{-1})): 417 (654), 343 (972). ATR-FTIR (cm^{-1}): 3069, 1593, 1576, 1556, 747. Anal. Calcd (found) for C$_{20}$H$_{18}$MnN$_2$: %C, 70.38 (69.29); %H, 5.28 (5.22); %N, 8.21 (8.74). Carbon percentages are consistently low despite several attempts.

Synthesis of 1-4,4′-Me$_2$bipy. The procedure and workup for 1-4,4′-Me$_2$bipy was the same as that for 1-bipy with the following modifications: 4,4′-dimethyl-2,2′-bipyridine (90 mg, 0.49 mmol), 1 (90 mg, 0.49 mmol). Yield: 30 mg, 17%.

Concentrated solutions of the adduct in THF stored at −35 °C afforded XRD quality crystals. UV-vis (THF) (ε = M^{-1} cm^{-1}): 420 (891), 341 (1388). ATR-FTIR (cm^{-1}): 3073, 3055, 1611, 1557, 1441, 762. Anal. Calcd (found) for C$_{22}$H$_{22}$MnN$_2$: %C, 71.54 (70.40); %H, 5.96 (5.83); %N, 7.58 (7.32). Carbon percentages are consistently low despite several attempts.

Synthesis of 1-6,6′-Me$_2$bipy. The procedure and workup for 1-6,6′-Me$_2$bipy was the same as that for 1-bipy with the following modifications: 6,6′-dimethyl-2,2′-bipyridine (91 mg, 0.49 mmol), 1 (90 mg, 0.49 mmol). Yield: 119 mg, 66%. Concentrated solutions of the adduct in THF stored at −35 °C afforded XRD quality crystals. UV-vis (THF) (ε = M^{-1} cm^{-1}): 415 (408). ATR-FTIR (cm^{-1}): 3069, 3029, 1597, 1576, 1443, 791. Anal. Calcd (found) for C$_{22}$H$_{22}$MnN$_2$: %C, 71.54 (71.31); %H, 6.00 (6.41); %N, 7.58 (7.25). μ_{eff} (benzene, 298 K) = 5.0μ_B.

Synthesis of 1-phen. The procedure and workup for 1-phen was the same as that for 1-bipy with the following modifications: 1,10-phenanthroline (95 mg, 0.53 mmol), 1 (95 mg, 0.53 mmol). Yield: 132 mg, 68%. Concentrated solutions of the adduct in toluene stored at −35 °C afforded XRD quality crystals. UV-vis (THF) (ε = M^{-1} cm^{-1}): 435 (1552). ATR-FTIR (cm^{-1}): 3062, 1621, 1575, 1513, 1421, 727. Anal. Calcd (found) for C$_{22}$H$_{18}$MnN$_2$: %C, 72.33 (69.07); %H, 4.97 (5.09); %N, 7.67 (6.81). Carbon percentages are consistently low despite several attempts.

Synthesis of 1-4,7-Ph$_2$phen. The procedure and workup for 1-4,7-Ph$_2$phen was the same as that for 1-bipy with the following modifications: 4,7-diphenyl-1,10-phenanthroline (187 mg, 0.56 mmol), 1 (102 mg, 0.55 mmol). Yield: 158 mg, 55%. Concentrated solutions of the adduct in THF stored at −35 °C afforded XRD quality crystals. UV-vis (THF) (ε = M^{-1} cm^{-1}): 468 (1039). ATR-FTIR (cm^{-1}): 3052, 3036, 1557, 1517, 1416, 760. Anal. Calcd (found) for C$_{34}$H$_{26}$MnN$_2$: %C, 78.91 (74.91); %H, 5.06 (5.29); %N, 5.41 (4.45). Carbon percentages are consistently low despite several attempts.

Synthesis of 1-2,9-Me$_2$phen. The procedure and workup for 1-2,9-Me$_2$phen was the same as that for 1-bipy with the following modifications: 2,9-dimethyl-1,10-phenanthroline (107 mg, 0.51 mmol), 1 (94 mg, 0.51 mmol). Yield: 115 mg, 57%. Concentrated solutions of the adduct in THF stored at −35 °C afforded XRD quality crystals. UV-vis (THF) (ε = M^{-1} cm^{-1}): 453 (341.36), 328 (1064). ATR-FTIR (cm^{-1}): 3046, 1591, 1560, 1501, 1424, 731. Anal. Calcd (found) for C$_{24}$H$_{22}$MnN$_2$: %C, 73.28 (73.58); %H, 5.64 (5.68); %N, 7.12 (7.08). μ_{eff} (benzene, 298 K) = 6.1μ_B.

Synthesis of 1-py$_2$. The procedure and workup for 1-py$_2$ was the same as that for 1-bipy with the following modifications: pyridine (80 μL, 1 mmol), 1 (90 mg, 0.49 mmol), bright yellow solution. Yield: 92 mg, 55%. Concentrated solutions of the adduct in toluene stored at −35 °C afforded XRD quality crystals. UV-vis (THF) (ε = M^{-1} cm^{-1}): featureless, shoulder 300 nm. ATR-FTIR (cm^{-1}): 3068, 3055, 1599, 1570, 1485, 1441, 759. Anal. Calcd (found) for C$_{20}$H$_{20}$MnN$_2$: %C, 69.97 (69.93); %H, 5.87 (5.90); %N, 8.16 (8.36). μ_{eff} (benzene, 298 K) = 5.1μ_B.

Synthesis of 1-terpy. The procedure and workup for 1-terpy was the same as that for 1-bipy with the following modifi-

cations: terpyridine (95 mg, 0.41 mmol) in toluene (5 ml) was added dropwise to a solution of **1** (75 mg, 0.41 mmol) in toluene (5 ml). Yield: 150 mg, 87%. Vapor diffusion of hexane into a saturated solution of **1**-terpy in THF afforded crystals suitable for XRD. UV-vis (THF) (ε = mol^{-1} cm^{-1}): 235 (26 680), 278 (17 958). ATR-FTIR (cm^{-1}): 3056, 1593, 1570, 1474, 770. Anal. Calcd (found) for $C_{25}H_{21}MnN_3$: %C, 71.77 (71.54); %H, 5.06 (5.53); %N, 10.04 (10.15).

%V_{bur} calculation. The SambVca 2.0 web application was used to calculate the %V_{bur} and also generate the steric maps. The *xyz* coordinate files were created using IQmol v2.7.1 for DFT structures or Mercury v3.9 for XRD determined structures. The sphere radius we employed was 3.5 Å and chosen based on the original work by Cavallo and Nolan.[27] Hydrogen atoms were included in the calculation of the %V_{bur}.

Conflicts of interest

The authors declare no competing financial interest.

Acknowledgements

Notes and references

1 G. Wilkinson, M. Rosenblum, M. C. Whiting and R. B. Woodward, *J. Am. Chem. Soc.*, 1952, **74**, 2125–2126.

2 R. R. Gagne, C. A. Koval and G. C. Lisensky, *Inorg. Chem.*, 1980, **19**, 2854–2855.

3 H. H. Brintzinger, D. Fischer, R. Mülhaupt, B. Rieger and R. M. Waymouth, *Angew. Chem., Int. Ed. Engl.*, 1995, **34**, 1143–1170.

4 G. Gasser, I. Ott and N. Metzler-Nolte, *J. Med. Chem.*, 2011, **54**, 3–25.

5 J. M. O'Connor and C. P. Casey, *Chem. Rev.*, 1987, **87**, 307–318.

6 W. Simanko, V. N. Sapunov, R. Schmid, K. Kirchner and S. Wherland, *Organometallics*, 1998, **17**, 2391–2393.

7 (*a*) G. Huttner, H. H. Brintzinger, L. G. Bell, P. Friedrich, V. Bejenke and D. Neugebauer, *J. Organomet. Chem.*, 1978, **145**, 329–333; (*b*) E. U. van Raaij, H. H. Brintzinger, L. Zsolnai and G. Huttner, *Z. Anorg. Allg. Chem.*, 1989, **577**, 217–222.

8 (*a*) L. F. Veiros, *Organometallics*, 2000, **19**, 5549–5558; (*b*) M. J. Calhorda, C. C. Romao and L. F. Veiros, *Chem. – Eur. J.*, 2002, **8**, 868–875.

9 R. A. Layfield, *Chem. Soc. Rev.*, 2008, **37**, 1098–1107.

10 M. E. Switzer and M. F. Rettig, *J. Chem. Soc., Chem. Commun.*, 1972, 687–688.

11 G. Wilkinson, F. A. Cotton and J. M. Birmingham, *J. Inorg. Nucl. Chem.*, 1956, **2**, 95–113.

12 (*a*) A. D. Bond, R. A. Layfield, J. A. MacAllister, M. McPartlin, J. M. Rawson and D. S. Wright, *Chem. Commun.*, 2001, 1956–1957; (*b*) C. S. Alvarez, A. Bashall, E. J. McInnes, R. A. Layfield, R. A. Mole, M. McPartlin, J. M. Rawson, P. T. Wood and D. S. Wright, *Chem. – Eur. J.*, 2006, **12**, 3053–3060.

13 F. Bottomley, P. N. Keizer and P. S. White, *J. Am. Chem. Soc.*, 1988, **110**, 137–140.

14 (*a*) C. D. Abernethy, A. H. Cowley, R. A. Jones, C. L. B. Macdonald, P. Shukla and L. K. Thompson, *Organometallics*, 2001, **20**, 3629–3631; (*b*) M. D. Walter, D. Baabe, M. Freytag and P. G. Jones, *Z. Anorg. Allg. Chem.*, 2016, **642**, 1259–1263.

15 J. Heck, W. Massa and P. Weinig, *Angew. Chem., Int. Ed. Engl.*, 1984, **23**, 722–723.

16 C. G. Howard, G. S. Girolami, G. Wilkinson, M. Thorntonpett and M. B. Hursthouse, *J. Am. Chem. Soc.*, 1984, **106**, 2033–2040.

17 J. W. Lauher and R. Hoffmann, *J. Am. Chem. Soc.*, 1976, **98**, 1729–1742.

18 (*a*) C. Soria Alvarez, A. Bashall, A. D. Bond, D. Cave, E. A. Harron, R. A. Layfield, M. E. G. Mosquera, M. McPartlin, J. M. Rawson, P. T. Wood and D. S. Wright, *Dalton Trans.*, 2003, 3002–3008; (*b*) C. S. Alvarez, S. R. Boss, J. C. Burley, S. M. Humphry, R. A. Layfield, R. A. Kowenicki, M. McPartlin, J. M. Rawson, A. E. Wheatley, P. T. Wood and D. S. Wright, *Dalton Trans.*, 2004, 3481–3487.

19 J. W. Faller, R. H. Crabtree and A. Habib, *Organometallics*, 1985, **4**, 929–935.

20 C. A. Tolman, *J. Am. Chem. Soc.*, 1970, **92**, 2956–2965.

21 C. A. Tolman, *Chem. Rev.*, 1977, **77**, 313–348.

22 T. E. Muller and D. M. P. Mingos, *Transition Met. Chem.*, 1995, **20**, 533–539.

23 S. S. Batsanov, *Inorg. Mater.*, 2001, **37**, 871–885.

24 A. Glockner, H. Bauer, M. Maekawa, T. Bannenberg, C. G. Daniliuc, P. G. Jones, Y. Sun, H. Sitzmann, M. Tamm and M. D. Walter, *Dalton Trans.*, 2012, **41**, 6614–6624.

25 (*a*) A. Poater, B. Cosenza, A. Correa, S. Giudice, F. Ragone, V. Scarano and L. Cavallo, *Eur. J. Inorg. Chem.*, 2009, **2009**, 1759–1766; (*b*) L. Falivene, R. Credendino, A. Poater, A. Petta, L. Serra, R. Oliva, V. Scarano and L. Cavallo, *Organometallics*, 2016, **35**, 2286–2293.

26 (*a*) A. C. Hillier, W. J. Sommer, B. S. Yong, J. L. Petersen, L. Cavallo and S. P. Nolan, *Organometallics*, 2003, **22**, 4322–4326; (*b*) A. Poater, F. Ragone, S. Giudice, C. Costabile, R. Dorta, S. P. Nolan and L. Cavallo, *Organometallics*, 2008, **27**, 2679–2681.

27 H. Clavier and S. P. Nolan, *Chem. Commun.*, 2010, **46**, 841–861.

28 A. Poater, F. Ragone, R. Mariz, R. Dorta and L. Cavallo, *Chem. – Eur. J.*, 2010, **16**, 14348–14353.

29 (*a*) M. Schmittel, A. Ganz, W. A. Schenk and M. Hagel, *Z. Naturforsch., B: J. Chem. Sci.*, 1999, **54**, 559–564; (*b*) M. D. Sampson, A. D. Nguyen, K. A. Grice, C. E. Moore, A. L. Rheingold and C. P. Kubiak, *J. Am. Chem. Soc.*, 2014, **136**, 5460–5471.

30 K. Kamata, A. Suzuki, Y. Nakai and H. Nakazawa, *Organometallics*, 2012, **31**, 3825–3828.

31 D. E. Stephens, J. Lakey-Beitia, J. E. Burch, H. D. Arman and O. V. Larionov, *Chem. Commun.*, 2016, **52**, 9945–9948.